Journal of ELECTRONIC MATERIALS, Vol. 50, No. 4, 2021
https://doi.org/10.1007/s11664-020-08567-z

ASIAN CONSORTIUM ACCMS–INTERNATIONAL CONFERENCE ICMG 2020

Effect of Alkoxy Side-Chains on Conjugated Polymer/Non-fullerene Acceptor Interfaces in Organic Solar Cells

SHEIK HASEENA[1] and MAHESH KUMAR RAVVA [1,2]

1.—Department of Chemistry, SRM University-AP, Amaravati, Andhra Pradesh 522508, India.
2.—e-mail: mahesh.r@srmap.edu.in

In this study, we have attempted to gain insights into the impact of alkoxy side-chains substituted on the end group of the non-fullerene acceptor. It has been shown by experimental studies that the length and position of these alkoxy side-chains substantially influence the power conversion efficiencies of solar cell devices. A detailed analysis has been made on how the length of the alkoxy side-chains impact the molecular packing and electronic and optical properties of conjugated polymers and non-fullerene acceptor blends using quantum chemical methods. The results obtained from this study provide information on why a particular alkoxy side-chain results in better device efficiencies.

Key words: Donor–acceptor complexes, non-fullerene acceptors, conjugated polymers, density functional theory

INTRODUCTION

Organic solar cells (OSCs) based on π-conjugated polymers and fullerene materials have many advantages over inorganic counterparts such as environmentally friendliness, solution processing, light weight, flexibility, and low cost.[1–4] The active layer of OSCs consists of electron donor and electron acceptor materials and usually has a decisive influence on the device performance. The π-conjugated polymers composed of alternating electron-rich and electron-poor units act as electron donor materials. Fullerene or its derivatives are used as electron acceptor materials. Several strategies have been developed to improve the performance of OSCs.[5–7] Energy level tuning between electron donor and electron acceptor materials and tuning the active layer's morphology results in power conversion efficiencies (PCEs) over 12%.[8] However, the PCEs of polymer-fullerene-based bulk-heterojunction solar cells (BHJs) are hindered by a few fundamental drawbacks of fullerene-based electron acceptor materials. The limitations of fullerenes and their derivatives as electron acceptor materials include weak absorption in the visible and near infra-red regions, high cost, and limited energy-level tunability, to name a few.

Non-fullerene-based electron acceptors (NFAs) have emerged as an alternative to fullerene derivatives.[9,10] The design and development of new NFAs offer the possibility of addressing the drawbacks of fullerene-based acceptors. Several types of NFA, such as rylene diimides and perylene diimide-based polymers and fused-ring electron acceptor molecules, are designed and used as electron acceptor materials.[11–13] Among these, the fused-ring electron acceptor receives considerable attention.[14] These fused-ring electron acceptor molecules consist of two electron-poor (end group) termini and an electron-rich unit (core group). The various alkyl or aryl side-chains are appended on the periphery of these molecules to increase miscibility. The energy levels and optical properties of these molecules can be varied by changing various combinations of electron-poor and electron-rich units.

Another main advantage of NFAs over fullerene derivatives is the ability to absorb light. The NFAs can be chosen in such a way that these molecules

(Received August 28, 2020; accepted October 13, 2020; published online November 12, 2020)

can absorb sunlight, which is complementary to the light-absorption range of donor materials. Thus, the active layer made up of a conjugated polymer and NFAs can absorb more sunlight and generate more charges. The donor materials absorb sunlight and form excitons on donor materials. The exciton dissociates into a hole and electron, and the photo-induced electron transfers from donor to acceptor material. Similarly, an exciton is formed on acceptor material that can dissociate into a hole and electron, and the hole transfers from acceptor to donor material. Hence, energy-level matching for both hole and electron transfer is critical for better charge generation.

Several research reports highlight the impact of end-groups and alkyl side-chains on device performance.[15–18] Zhan et al. developed an acceptor–donor–acceptor type fused-ring acceptor, viz., 3,9-bis(2-methylene-(3-(1,1-dicyanomethylene)-indanone))-5,5,11,11-tetrakis(4-hexyl phenyl)-dithieno-sindaceno dithiophene (ITIC).[19] It is shown that the performance of organic solar cells is influenced by the position and length of alkoxy side-chains on the end-group of NFAs. Li et al. synthesized several ITIC derivatives by altering the position of methoxy groups.[17] It is found that even the position of methoxy groups on NFAs has a substantial impact on power conversion efficiencies (PCEs). A few computational studies have been performed to gain insights into the impact of alkyl side-chains on the PCEs of organic solar cells. Wang et al. performed combined molecular dynamics (MD) simulations and density functional theory (DFT) calculations to understand the influence of the position of the methoxy group and concluded that substitution position in the end group impacted the intermolecular packing and electron-transfer properties.[15] Recently, Zhu et al. synthesized new ITIC isomers by varying the length of alkoxyl side-chain length at the second position of the end group.[16] Interestingly, increasing the length of the alkoxy side-chain from methoxy to butoxy decreases organic photovoltaics (OPV) performance with the poly(2,6-(4,8-bis(5-(2-ethylhexyl)thiophen-2-yl)benzo1,2-b:4,5-b′-dithiophen)-co-(1,3-di(5-thiophene-2-yl)-5,7-bis (2-ethylhexyl)benzo1,2-c:4,5-c′dithiophene-4,8-dione) (PBDBT) polymer. We noted from these studies that both open-circuit and fill-factors are constant irrespective of position and length of alkoxy side-chains on the end group of NFA. Only short-circuit currents are substantially impacted the PCE. It is important to understand at the molecular level how subtle side-chain tuning influences organic solar cell performance. In this study, we have attempted to study the influence of alkoxy side-chains substituted on end-groups of electron acceptor molecules that impact the polymer/non-fullerene acceptor packing using DFT methods. The electronic properties of isolated NFAs and polymer-NFA complexes are studied in detail. Wherever possible, our results are compared with the experimental results.

COMPUTATIONAL METHODOLOGY

In order to understand the impact of alkoxy chain length on the performance of OPVs, we have considered five NFA ITIC derivatives such as ITIC with hydroxy chain (ITOH), ITIC with methoxy chain (ITOMe), ITIC with propoxy chain (ITOPr), and ITIC with butoxy chain (ITOBu). A tetramer of a PBDBT oligomer is considered as donor polymer. The chemical structures of various ITIC derivatives and the PBDBT polymer considered in this study are shown in Fig. 1. Geometry optimizations of isolated ITIC derivative molecules with different alkyl side-chain lengths and a tetramer of the PBDBT oligomer were optimized at the B3LYP/6-31g** level of theory. Five different combinations of polymer-NFA complexes are considered. These are PBDBT:ITOH, PBDBT:ITOMe, PBDBT:ITOPr, and PBDBT:ITOBu. As the geometries of these complexes are sensitive to the initial geometry, 15 random geometries were generated in each case using Packmol code.[20] All polymer-NFA complexes with long alkyl side-chains were fully optimized using the PM7 method implemented in the MOPAC program.[21] It is shown that the performance of PM7 is comparable with the DFT methods.[22,23] The optimized geometries are further used to study various electronic and optical properties using density functional theory (DFT)-based methods. Excited-state analysis has been carried out at the TD-B3LYP/6-31G** level of theory using the PM7 optimized geometries. The hole–electron distance and calculated charge density difference (CDD) maps were obtained using Multiwfn software.[24] All DFT calculations were performed using Gaussian 16 package.[25]

RESULTS AND DISCUSSION

We start our discussion with the electronic properties of isolated non-fullerene acceptors. The optimized geometries reveal that the backbone of these acceptors is planar. The calculated wave functions of the highest occupied molecular orbital (HOMO) and lowest unoccupied orbital molecular orbital (LUMO) for all NFAs considered in this study are depicted in Fig. 2. As expected, the substitution of alkoxy chains on the end group has a minor impact on the HOMO and LUMO values. It is also worth noting that the calculated HOMO and LUMO values of these NFAs are in good agreement with the experimental ionization potentials and electron affinity values.[16] The HOMO wave function is localized on the electron-rich unit of NFAs, whereas the LUMO wave function is delocalized on the entire backbone. To gain more insight into the impact of alkoxy chain substitution on the end group, we have also calculated the hole reorganization and electron reorganization energies of all NFAs. The calculated hole and electron reorganization energies are reported in Table I. As the LUMO wavefunction delocalized on both electron-rich and

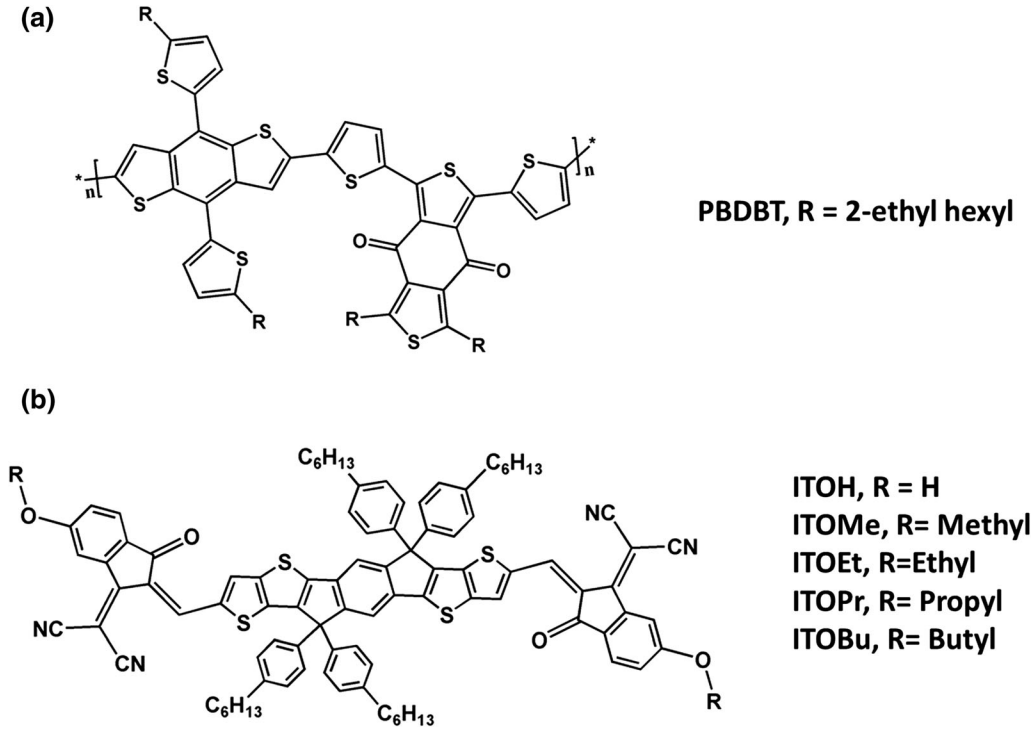

Fig. 1. Chemical structures of PBDBT with alkyl side-chain pattern (top) and various non-fullerene acceptors, viz., ITOH, ITOMe, ITOEt, ITOPr, and ITOBu (bottom).

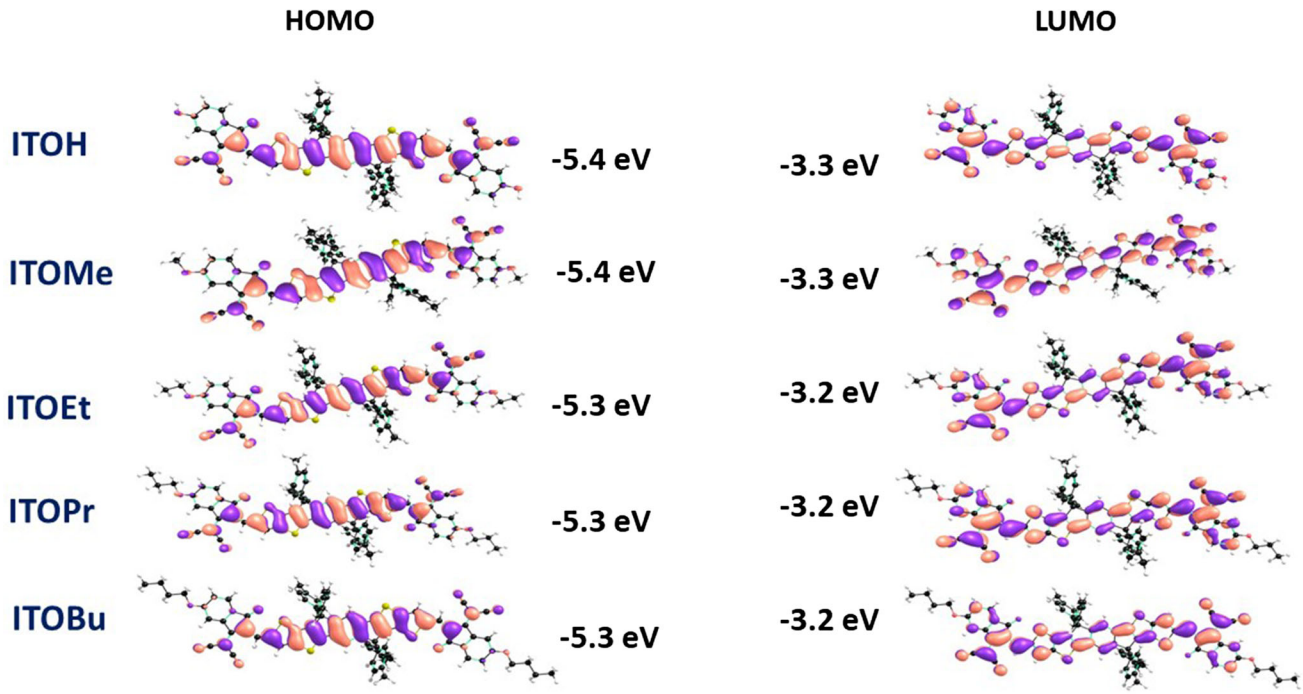

Fig. 2. Pictorial representation of the HOMO wave functions (left) and LUMO wave functions (right) of various non-fullerene acceptors as determined at the B3LYP/6-31G(d,p) level of theory. HOMO and LUMO energy values (in eV) are also given.

electron-poor units, the calculated electron reorganization energies are smaller than other NFAs reported in the literature.[26] Also, it is possible to observe from these values that the alkyl chains on the end group have minimal or no impact on the electronic properties of isolated NFA molecules.

We have also calculated the excited-state energies of the PBDBT oligomer and NFA molecules such as ITOH, ITOMe, ITOEt, ITOPr, and ITOBu

Table I. Calculated HOMO and LUMO energy values, HOMO–LUMO gap (E_g), hole reorganization, electron reorganization energies, lowest excitation energy values of various ITIC derivatives using B3LYP/6-31G(d,p) level of theory

	B3LYP/6-31G*			Experimental[a]			Hole reorganization (in meV)	Electron reorganization (in meV)	S_1 (in eV)
	HOMO	LUMO	E_g	HOMO	LUMO	E_g			
ITOH	− 5.38	− 3.29	2.09	–	–		170.0	152.6	1.88
ITOMe	− 5.35	− 3.25	2.10	− 5.50	− 3.76	1.74	179.0	159.0	1.88
ITOEt	− 5.33	− 3.23	2.10	− 5.49	− 3.86	1.63	181.0	161.2	1.88
ITOPr	− 5.32	− 3.23	2.09	− 5.52	− 3.80	1.72	180.0	161.2	1.88
ITOBu	− 5.32	− 3.22	2.10	− 5.49	− 3.81	1.68	180.0	162.2	1.88

All values are given in eV. Experimental values are also given for comparison.
[a]Values are taken from Zhu et al.[16]

considered in this study. The calculated excited energies are reported in Table I. All these values are in close agreement with the experimental values.[16] All of the acceptor molecules have more or less the same lowest excitation energies. These results clearly show that the length of the alkoxy group has no impact on the isolated NFA molecules. It is also worth mentioning that the absorption values of the oligomer and NFAs have complementary absorption. Thus, the blends made from these polymer and NFA combinations may cover a significant portion of the solar spectrum. The calculated electronic and optical energies clearly show the energy level matching between donor oligomer and NFA molecules.

Packing Between PBDBT Oligomer and ITIC Derivatives

We studied the impact of the length of alkoxy side-chains on the packing between the PBDBT oligomer and NFA molecule by generating different oligomer and NFA complexes. As described in the computational methods section, five different combinations of PBDBT:NFA complexes such as PBDBT:ITIOH, PBDBT:ITOMe, PBDBT:ITOEt, PBDBT:ITOPr, and PBDBT:ITOBu are considered. Since PBDBT chains and NFA molecules can interact in several ways, we have considered 15 random initial geometries in each case, and all geometries are fully optimized using the PM7 method. The interaction between the PBDBT oligomer and NFA molecule strongly depends on the interaction between the PBDBT oligomer backbone and NFA molecule backbone, alkyl side-chains on the PBDBT oligomer and NFA molecule backbone, and alkyl side-chains on NFA molecules with alkyl side-chains on the PBDBT oligomer. We found twists in the dihedral angle between electron-rich and electron-poor units in the NFA molecules upon interaction with a donor oligomer.

Donor and acceptor blends with cascading energy levels provide a driving force for charge transfer (CT) state.[27,28] The driving force of electron charge transfer comes from ΔLUMO = ($LUMO_D$-$LUMO_A$). Similarly, the driving force for the hole charge transfer results from ΔHOMO = ($HOMO_D$-$HOMO_A$). It has been previously proposed that effective hole/electron transfer requires a ΔLUMO/ΔHOMO value higher than the exciton binding energy of the intramolecular exciton in donor–acceptor material. The excited state energies and HOMO and LUMO energy values for all combinations of donor–acceptor blends such as PBDBT:ITOH, PBDBT:ITOMe, PBDBT:ITOEt, PBDBT:ITOPr, and PBDBT:ITOBu are reported in supporting information Tables S1–S5. The calculated ΔHOMO and ΔLUMO values for PBDBT:ITOBu complexes are ∼ 75 meV and 875 meV, respectively. These values for the PBDBT:ITICOMe complexes are ∼ 80 meV and 900 meV, respectively. It is worth mentioning that HOMO energy offset values are very small compared to LUMO energy offset values. Even though there is a small energy offset between the energy levels, good charge generation was observed in the blends. It is still not clear why NFA-based OSC exhibits high charge generation despite a relatively small energy offset. However, we believe the small energy offset values and strong electronic couplings between HOMO of PBDBT and HOMO of NFA molecules are responsible for the efficient charge generation. We have calculated the electronic coupling values for all donor–acceptor blends such as PBDBT:ITOH, PBDBT:ITOMe, PBDBT:ITOEt, PBDBT:ITOPr, and PBDBT:ITOBut complexes. We found that in all cases, LUMO–LUMO electronic couplings are stronger (∼ 20 meV) than the HOMO–HOMO couplings (∼ 10 meV) (all electronic coupling values are given in supporting information Table S6). Overall, strong electronic couplings and small $HOMO_D$–$HOMO_A$ results in good charge generation in these

systems. It is worth mentioning that these findings are in agreement with the experimental results.[16]

Excited-State Analysis on the Complexes of PBDBT Oligomer and ITIC Derivatives

We have calculated the excitation energies of donor–acceptor complexes obtained from optimized geometries. All values are reported in supporting information Tables S1 to S5. As mentioned before, in each PBDBT:NFA combination, we have 15 complexes. Instead of reporting individual energies for each complex in five different combinations, we have reported the average value and the standard deviation. All these values are given Table II. NFA (S1) and PBDBT (S1) correspond to the lowest excitation energies and the nature of the excitation state in local-type excitation. CT state energy corresponds to the energy of charge transfer state for PBDBT:NFA complexes. In the CT state, holes localizes on PBDBT oligomers, and electrons localize on ITIC derivative molecules (shown in Fig. 3). From Table II, it is possible to observe the following points: Among all complexes, in the PBDBT:ITOMe complex, the standard deviation value for NFA (S1) is around 90 meV. In all other cases, the same value is 130-170 meV. We defined the standard deviation value as the energetic disorder in the system. Generally, in the case of organic semiconductors, energetic disorder plays a crucial role in the charge transport properties and the performance of solar cells.[29,30] Even though the number of configurations that we considered here is small, the results obtained from this analysis provide insight into the static energy disorder in the non-fullerene acceptor molecules. As we mentioned before, the isolated NFA molecules are planar in the isolated state. However, when they interact with the PBDBT oligomer chain, we observed twists in the backbone. The structural changes (especially dihedral angles between fused rings) lead to variation in their lowest excitation energies. Since we have calculated the excited state energies of NFA molecules extracted from the various combinations of PBDBT:NFA donor–acceptor interfaces, we obtained a distribution of energy values rather than a single value. From this analysis, one can observe that the ITOMe molecule shows less structural variation and thus exhibits less energetic disorder. This might be due to the presence of simple methoxy group substitution on the end group. Other cases such as ITOEt, ITOPr, and ITOBu show more disorder due to interactions between long alkoxy chains and oligomer chains. It is previously shown that disorder present in the system leads to energy loss and charge recombination.[31] In the case of PBDBT:ITOMe, a small energy difference between NFA (S1) and ECT is observed. Overall, the alkoxy chains substituted on the end group of NFA molecules impact NFA structure, especially when it interacted with the PBDBT oligomer chain. Hence, we observe more energetic disorder in the systems where alkoxy chains are longer.

CONCLUSIONS

We have demonstrated the impact of alkoxy side-chain length on the end group of non-fullerene acceptors on molecular packing, electronic, and optical properties using a density functional theory-based B3LYP method. Results clearly show that the isolated ITIC derivatives (ITOH, ITOMe, ITOEt, ITOPr, and ITOBu) have a planar backbone. The substitution of alkoxy groups on the end group has minimal to no impact on the electronic and optical properties of isolated acceptor molecules. The impact of alkoxy chains on packing between polymer and acceptor interfaces is demonstrated by considered various combinations of donor polymer with various ITIC derivatives. Acceptor molecules interact with conjugated polymer backbone, due to interactions between alkyl side-chains of PBDBT donor oligomer and side-chains of non-fullerene acceptor and interactions between side-chains of non-fullerene acceptor with PBDBT oligomer backbone. We observed substantial structural and

Table II. Calculated average and standard deviation values for charge transfer state energies of various PBDBT:ITIC derivatives complexes, and lowest excitation values of NFA molecules and PBDBT oligomer in the complexes

Complexes	S1@ NFA (eV)	S1 @ PBDBT (eV)	CT state (eV)
PBDBT:ITOH	1.73 ± 0.17	2.60 ± 0.17	1.64 ± 0.17
PBDBT:ITOMe	1.81 ± 0.09	2.69 ± 0.11	1.78 ± 0.20
PBDBT:ITOEt	1.75 ± 0.22	2.53 ± 0.15	1.73 ± 0.20
PBDBT:ITOPr	1.79 ± 0.17	2.32 ± 0.52	1.61 ± 0.35
PBDBT:ITOBu	1.81 ± 0.13	2.45 ± 0.39	1.74 ± 0.13

All values are calculated using TD-B3LYP/6-31G(d,p) level of theory. All values are given in eV.

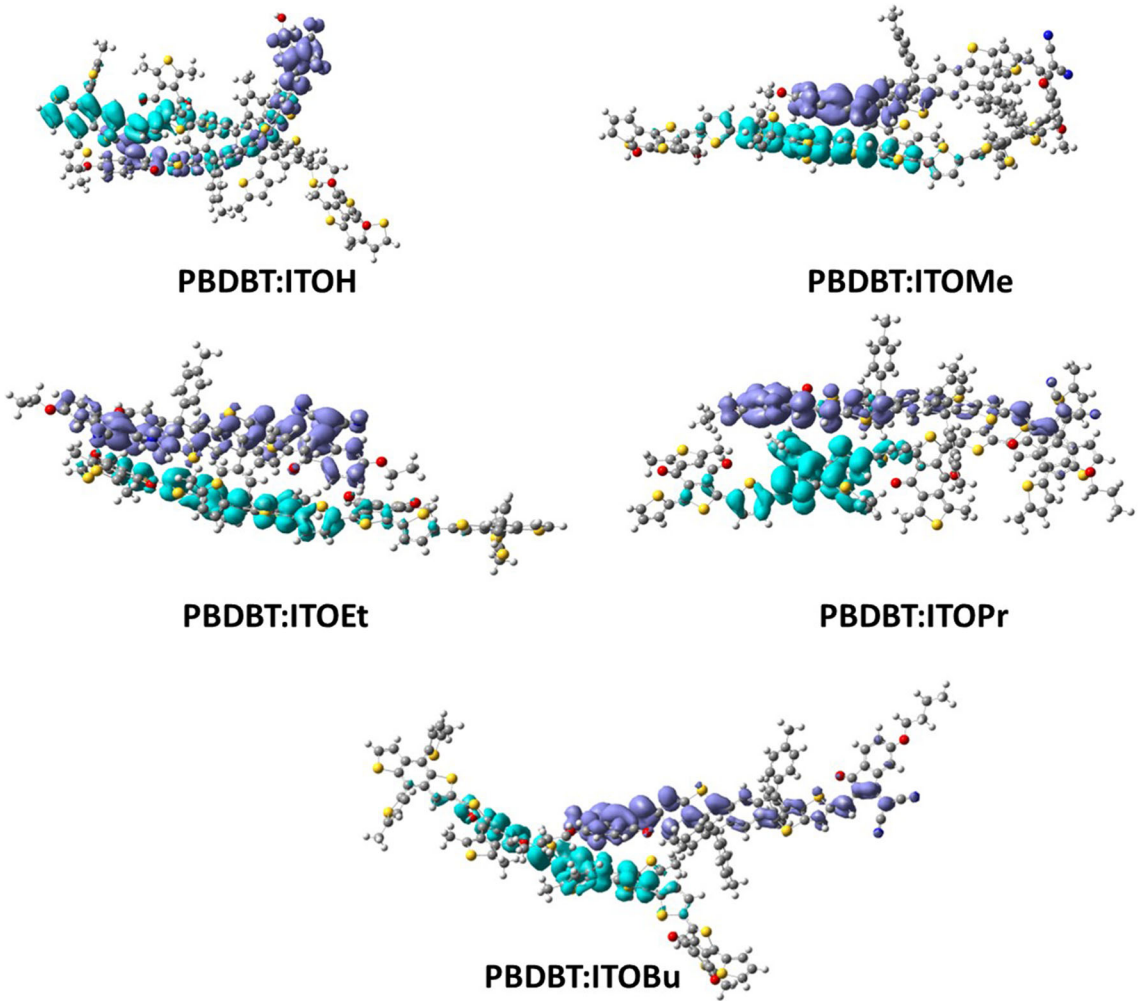

Fig. 3. Charge density difference maps of various representative PBDBT:NFA blends as determined at the B3LYP/6-31G(d,p) level of theory. Blue and cyan represent electrons and holes, respectively.

energy level variations in acceptor cases with long alkoxy side-chains on the end group. In the case of acceptors with methoxy side-chains (ITOMe), less variation in the energy levels is observed. The previous experimental studies found that the acceptors with methoxy side-chains have shown high short-circuit currents and higher PCEs than the longer alkoxy side-chains. Overall, smaller energy level variations in PBDBT:ITOMe blends suppress the energy loss and charge recombination and show higher PCEs.

ACKNOWLEDGMENTS

We thank the Department of Science and Technology (DST), New Delhi, India, for supporting this research under the DST-INSPIRE scheme (DST/INSPIRE/04/2017/001393). We would like to thank SRM Supercomputer Center, SRM Institute of Science and Technology for providing the computational facility.

CONFLICT OF INTEREST

The authors declare that they have no conflict of interest.

ELECTRONIC SUPPLEMENTARY MATERIAL

The online version of this article (https://doi.org/10.1007/s11664-020-08567-z) contains supplementary material, which is available to authorized users.

REFERENCES

1. N.S. Sariciftci, L. Smilowitz, A.J. Heeger, and F. Wudl, *Science* 258, 1474 (1992).
2. J.-L. Brédas, J.E. Norton, J. Cornil, and V. Coropceanu, *Acc. Chem. Res.* 42, 1691 (2009).

3. G. Yu, J. Gao, J.C. Hummelen, F. Wudl, and A.J. Heeger, *Science* 270, 1789 (1995).
4. A.J. Heeger, *Adv. Mater.* 26, 10 (2014).
5. Y. Li, *Acc. Chem. Res.* 45, 723 (2012).
6. Y. Lin, J. Wang, Z.-G. Zhang, H. Bai, Y. Li, D. Zhu, and X. Zhan, *Adv. Mater.* 27, 1170 (2015).
7. Y. Liu, J. Zhao, Z. Li, C. Mu, W. Ma, H. Hu, K. Jiang, H. Lin, H. Ade, and H. Yan, *Nat. Commun.* 5, 5293 (2014).
8. M. Li, K. Gao, X. Wan, Q. Zhang, B. Kan, R. Xia, F. Liu, X. Yang, H. Feng, W. Ni, Y. Wang, J. Peng, H. Zhang, Z. Liang, H.-L. Yip, X. Peng, Y. Cao, and Y. Chen, *Nat. Photon.* 11, 85 (2017).
9. L. Zhan, S. Li, T.-K. Lau, Y. Cui, X. Lu, M. Shi, C.-Z. Li, H. Li, J. Hou, and H. Chen, *Energy Environ. Sci.* 13, 635 (2020).
10. Y. Cui, H. Yao, J. Zhang, K. Xian, T. Zhang, L. Hong, Y. Wang, Y. Xu, K. Ma, C. An, C. He, Z. Wei, F. Gao, and J. Hou, *Adv. Mater.* 32, 1908205 (2020).
11. B. Yadagiri, K. Narayanaswamy, S. Revoju, B. Eliasson, G.D. Sharma, and S.P. Singh, *J. Mater. Chem. C* 7, 709 (2019).
12. X. Long, Z. Ding, C. Dou, J. Zhang, J. Liu, and L. Wang, *Adv. Mater.* 28, 6504 (2016).
13. C. Li and H. Wonneberger, *Adv. Mater.* 24, 613 (2012).
14. A. Wadsworth, M. Moser, A. Marks, M.S. Little, N. Gasparini, C.J. Brabec, D. Baran, and I. McCulloch, *Chem. Soc. Rev.* 48, 1596 (2019).
15. T. Wang and J.-L. Brédas, *Adv. Funct. Mater.* 29, 1806845 (2019).
16. J. Zhu, S. Li, X. Liu, H. Yao, F. Wang, S. Zhang, M. Sun, and J. Hou, *J. Mater. Chem. A* 5, 15175 (2017).
17. S. Li, L. Ye, W. Zhao, S. Zhang, H. Ade, and J. Hou, *Adv. Energy Mater.* 7, 1700183 (2017).
18. S.A. Ayoub and J.B. Lagowski, *Phys. Chem. Chem. Phys.* 21, 23978 (2019).
19. W. Zhao, D. Qian, S. Zhang, S. Li, O. Inganäs, F. Gao, and J. Hou, *Adv. Mater.* 28, 4734 (2016).
20. L. Martínez, R. Andrade, E.G. Birgin, and J.M. Martínez, *J. Comput. Chem.* 30, 2157 (2009).
21. J.J.P. Stewart, *J. Mol. Model.* 13, 1173 (2007).
22. L. Wilbraham, E. Berardo, L. Turcani, K.E. Jelfs, and M.A. Zwijnenburg, *J. Chem. Inf. Model.* 58, 2450 (2018).
23. C. Sikorska and T. Puzyn, *Nanotechnology* 26, 455702 (2015).
24. T. Lu and F. Chen, *J. Comput. Chem.* 33, 580 (2012).
25. M. J. Frisch, G. W. Trucks, H. B. Schlegel, G. E. Scuseria, M. A. Robb, J. R. Cheeseman, G. Scalmani, V. Barone, G. A. Petersson, H. Nakatsuji, X. Li, M. Caricato, A. V. Marenich, J. Bloino, B. G. Janesko, R. Gomperts, B. Mennucci, H. P. Hratchian, J. V. Ortiz, A. F. Izmaylov, J. L. Sonnenberg, Williams, F. Ding, F. Lipparini, F. Egidi, J. Goings, B. Peng, A. Petrone, T. Henderson, D. Ranasinghe, V. G. Zakrzewski, J. Gao, N. Rega, G. Zheng, W. Liang, M. Hada, M. Ehara, K. Toyota, R. Fukuda, J. Hasegawa, M. Ishida, T. Nakajima, Y. Honda, O. Kitao, H. Nakai, T. Vreven, K. Throssell, J. A. Montgomery Jr., J. E. Peralta, F. Ogliaro, M. J. Bearpark, J. J. Heyd, E. N. Brothers, K. N. Kudin, V. N. Staroverov, T. A. Keith, R. Kobayashi, J. Normand, K. Raghavachari, A. P. Rendell, J. C. Burant, S. S. Iyengar, J. Tomasi, M. Cossi, J. M. Millam, M. Klene, C. Adamo, R. Cammi, J. W. Ochterski, R. L. Martin, K. Morokuma, O. Farkas, J. B. Foresman, and D. J. Fox, *Gaussian 16 Rev. C.01* (Wallingford, CT, 2016).
26. S.M. Swick, W. Zhu, M. Matta, T.J. Aldrich, A. Harbuzaru, J.T. Lopez Navarrete, R. Ponce Ortiz, K.L. Kohlstedt, G.C. Schatz, A. Facchetti, F.S. Melkonyan, and T.J. Marks, *Proc. Natl. Acad. Sci.* 115, E8341 (2018).
27. T.M. Clarke and J.R. Durrant, *Chem. Rev.* 110, 6736 (2010).
28. M.C. Scharber, D. Mühlbacher, M. Koppe, P. Denk, C. Waldauf, A.J. Heeger, and C.J. Brabec, *Adv. Mater.* 18, 789 (2006).
29. Y.L. Lin, M.A. Fusella, and B.P. Rand, *Adv. Energy Mater.* 8, 1702816 (2018).
30. N.R. Tummala, Z. Zheng, S.G. Aziz, V. Coropceanu, and J.-L. Brédas, *J. Phys. Chem. Lett.* 6, 3657 (2015).
31. A. Yin, D. Zhang, S.H. Cheung, S.K. So, Z. Fu, L. Ying, F. Huang, H. Zhou, and Y. Zhang, *J. Mater. Chem. C* 6, 7855 (2018).